Published in final edited form as:
Neurogastroenterol Motil. 2010 October ; 22(10): 1132–e290. doi:10.1111/j.1365-2982.2010.01546.x.

A murine model for the study of edema induced intestinal contractile dysfunction

Shinil K. Shah, DO[1,2], **Stacey D. Moore-Olufemi, MD**[1,2], **Karen S. Uray, PhD**[1,2,3], **Fernando Jimenez, MS**[1], **Peter A. Walker, MD**[1,2], **Hasen Xue, MD**[1], **Randolph H. Stewart, DVM, PhD**[3], **Glen A. Laine, PhD**[3], and **Charles S. Cox Jr, MD**[1,2,3]

[1] Department of Pediatric Surgery, University of Texas Medical School at Houston, Houston, Texas

[2] Department of Surgery, University of Texas Medical School at Houston, Houston, Texas

[3] Michael E. DeBakey Institute for Comparative Cardiovascular Science and Biomedical Devices, Texas A & M University, College Station, Texas

Abstract

Background—We have published extensively regarding the effects of edema on intestinal contractile function. However, we have found the need to expand our model to mice to take advantage of the much larger arsenal of research support, especially in terms of transgenic mouse availability and development. To that end, we have developed and validated a hydrostatic intestinal edema model in mice.

Methods—Male C57 Black 6 mice were subjected to a combination of high volume crystalloid resuscitation and mesenteric venous hypertension in an effort to induce hydrostatic intestinal edema. Wet to dry ratios, myeloperoxidase activity, mucosal injury scoring, STAT-3 nuclear activation, phosphorylated STAT-3 levels, NF-kappa B nuclear activation, myosin light chain phosphorylation, intestinal contractile activity, and intestinal transit were measured to evaluate the effects of the model.

Key Results—High volume crystalloid resuscitation and mesenteric venous hypertension resulted in the development of significant intestinal edema without an increase in myeloperoxidase activity or mucosal injury. Edema development was associated with increases in STAT-3 and NF-kappa B nuclear activation as well as phosphorylated STAT-3. There was a decrease in myosin light chain phosphorylation, basal and maximally stimulated intestinal contractile activity, and intestinal transit.

Conclusions & Inferences—Hydrostatic edema in mice result in activation of a signal transduction profile that culminates in intestinal contractile dysfunction. This novel model allows for advanced studies into the pathogenesis of hydrostatic edema induced intestinal contractile dysfunction.

MeSH Keywords

Edema; Ileus; Intestines; Murine; Resuscitation; Trauma

Please address all inquiries to: Charles S. Cox, Jr., MD, Department of Pediatric Surgery, University of Texas Medical School at Houston, 6431 Fannin Street, MSB 5.236, Houston, TX 77030, Phone: (713) 500-7307, Fax: (713) 500-7296, Charles.S.Cox@uth.tmc.edu.

COMPETING INTERESTS: The authors have no competing interests.

AUTHOR CONTRIBUTIONS: All authors contributed to study conception and design, acquisition, analysis and interpretation of data, drafting and critical revision of the manuscript, and approved the final submitted manuscript.

Introduction

The pathogenesis of small intestine contractile dysfunction in trauma patients is complex and has numerous underlying etiologies. Contributing pathophysiological processes include intra-abdominal sepsis, inflammation, and ischemia/reperfusion. A common end element intertwined between these causative factors is intestinal edema. Additively, strategies frequently used in the initial management of trauma patients, such as high volume crystalloid administration and intra-abdominal packing, alter oncotic and hydrostatic forces leading to net accumulation of tissue water.

Intestinal edema is often viewed as an inevitable consequence of both pathology and treatment, with little attention paid to its potential consequences as an amplifier or initiator of dysfunctional signaling cascades culminating in intestinal contractile dysfunction. Indeed, our group has been able to demonstrate that hydrostatic intestinal edema not associated with classic inflammatory factors, infection, or ischemia/reperfusion mediated injury results in early activation of signal transduction cascades classically attributed to models of global or regional ischemia/reperfusion, inflammation, and sepsis. Additionally, we have demonstrated that hydrostatic edema alters myosin light chain phosphorylation, the obligatory step in the intestinal contractile complex, leading to decreased intestinal contractility and ileus. (1–4)

A limitation of our work, however, has been the study subject, i.e., a rat model of hydrostatic intestinal edema. Although we have been able to further our understanding of the effects of edema on intestinal contractile function, we have found the need to expand our model to mice to take advantage of the much larger arsenal of research support, especially in terms of knock out model technology availability and development. In this manuscript, we detail the development and validation of a hydrostatic intestinal edema model in mice; specifically, we hypothesize that the combination of non-occlusive mesenteric venous hypertension (to mimic intra-abdominal packing) and high volume crystalloid resuscitation will result in development of significant intestinal edema and result in a similar signal transduction profile and end organ behavior as we have noted in rats.

Materials & Methods

All procedures were approved by the University of Texas Medical School at Houston Animal Welfare Committee and were consistent with the National Institutes of Health's *Guide for the Care and Use of Laboratory Animals* (HSC-AWC-07-031).

Animal Model

Male C57 Black 6 mice (6–7 weeks, 17–21 grams) were obtained from Harlan Laboratories, Inc (Houston, TX). Prior to experimentation, the animals were allowed to acclimate for at least 5 days in a temperature controlled environment with 12 hour alternating light/dark cycles. The mice were fasted for 12–16 hours (with free access to water) prior to experimentation. The mice were anesthetized with isoflurane. A midline laparotomy was performed. The superior mesenteric vein was carefully dissected free from its mesenteric attachments without significant manipulation of the small bowel. Animals were subsequently divided into CONTROL and EDEMA groups. CONTROL animal groups had brief exteriorization of the small bowel without manipulation and the laparotomy wound closed with 5-0 Vicryl suture.

EDEMA groups animals had induction of intestinal edema based on principles developed from our previously developed rat model of hydrostatic intestinal edema and included high

volume crystalloid resuscitation and induction of mesenteric venous hypertension (to mimic abdominal (specific peri-hepatic) packing. (2) Mesenteric venous hypertension was accomplished by placing a 4-0 silk suture around the superior mesenteric vein and subsequently tying it over a 2-0 sized stainless steel wire. The wire was removed, creating a non-occlusive outflow stricture which leads to a sustained increased in mesenteric venous pressure. By tying the suture over 2-0 sized stainless steel wire and subsequently removing the wire after the knot is tied down, we ensure that the superior mesenteric vein is not completely occluded. This was followed by closure of the laparotomy wound. 80 cc/kg of crystalloid (0.9% normal saline suture) was then administered slowly over 1 minute via subcutaneous infusion. The animals were then allowed to recover and were sacrificed at 30 minutes, 2 hours, or 6 hours. The ileum was used for all molecular analyses.

Wet to Dry Ratio

To confirm development of significant intestinal edema, wet to dry ratios were measured. After gently flushing the intraluminal contents of the proximal (i.e., duodenum and jejunum) small bowel, the bowel was gently milked dry and its wet weight was immediately measured. The small bowel was subsequently placed in a 60°C oven and allowed to dry over 2–3 days, until the dry weight was constant. Tissue water was then determined from the following equation.

$$\text{Wet to Dry Ratio} = [\text{wet weight} - \text{dry weight}]/\text{dry weight} \quad \text{Equation 1}$$

Acute Mesenteric Venous Hypertension

A separate set of mice underwent cannulation of the distal superior mesenteric vein for determination of baseline mesenteric venous pressures. To evaluate the effects of partial, non-occlusive elevation of mesenteric venous pressure, a distal mesenteric vein was cannulated immediately after constriction of the superior mesenteric vein to evaluate the degree of acute mesenteric venous hypertension. All measurements were performed using a pressure transducer connected to a Hewlett Packard monitor/terminal (78534B, Palo Alto, CA).

Preparation of Nuclear and Cytoplasmic Extracts

Frozen tissue was ground with a mortar and pestle over liquid nitrogen. Cytoplasmic and nuclear extracts were prepared using a commercially available nuclear extract kit (Active Motif, Carlsbad, CA) following the manufacturer's suggested protocol. Briefly, samples (ground tissue) were homogenized with a polytron in cold hypotonic buffer containing protease inhibitors (Protease Inhibitor Cocktail, Sigma Aldrich, St. Louis, MO) and phosphatase inhibitors (2 mM orthovanadate and 2 mM sodium fluoride). The homogenized samples were incubated at 4°C for 15 minutes and then centrifuged at 850 x *g* at 4°C for 10 minutes. The supernatant was saved. The residual pellet was re-suspended in cold hypotonic buffer containing protease and phosphatase inhibitors and incubated on ice for 15 minutes. After the addition of 0.05% detergent (Nonidet P-40), the samples were vortexed briefly and centrifuged at 14,000 x *g* at 4°C for 10 minutes. The supernatant was saved and combined with the first supernatant and called the cytoplasmic extract. The pellet was resuspended in lysis buffer, vortexed for 30 seconds, and incubated on ice for 30 minutes. The samples were then centrifuged at 14,000 x *g* at 4°C for 10 minutes. The resultant supernatant was called the nuclear extract. All samples were aliquotted and stored at −80°C.

Myeloperoxidase Activity

Myeloperoxidase activity was measured in cytoplasmic extracts from seromuscular samples as previously published. (5) Briefly, samples were diluted 1:5 and added to a 96 well plate and incubated with 100 microliters of SureBlue™ tetramethylbenzidine (TMB) microwell peroxidase substrate (KPL, Gaithersburg, MD) for 20 minutes at 37°C. The reaction was stopped by addition of 100 microliters of TMB Stop Solution (KPL, Gaithersburg, MD), and the optical density was measured at 450 nm. Each sample was assayed in duplicate, and the values were normalized to protein concentration (as determined by the Quick Start Bradford protein assay, Bio Rad, Hercules, CA).

Chiu Scoring

Full thickness segments from the distal ileum were fixed in buffered 10% formalin for at least 24 hours. After tissue processing, the tissue was embedded in paraffin and cut into approximately 7 μM slices and placed on glass microscope slides. After deparaffinization, they were then stained with hematoxylin (Hematoxylin Solution, Gill Number 2, Sigma Aldrich, St. Louis, MO) and eosin (Eosin Y Solution, Alcoholic, Sigma Aldrich, St. Louis, MO) according to the manufacturer's suggested protocol. The stained tissues were examined using light microscopy by a blinded investigator and scored from 1–5 utilizing the system as described by Chiu et al; grade 0, normal mucosa; grade 1, subepithelial space developing at the tip of the villus; grade 2, lifting of the epithelial layer from the lamina propria and moderate extension of the subepithelial space; grade 3, some denuded tips of the villi and massive lifting of the epithelial layer; grade 4, dilated and exposed capillaries and denuded villi; and grade 5, hemorrhage, ulceration, and disintegrated lamina propria. (6)

STAT-3 Nuclear Activation

Nuclear STAT-3 activation was measured in nuclear extracts of the ileum using a commercially available STAT-3 transcription factor assay kit (TransAm STAT-3, Active Motif, Carlsbad, CA) following the manufacturer's suggested protocol. Briefly, nuclear extracts were added to a 96-well plate in which the oligonucleotide containing the STAT-3 consensus binding site was immobilized. After incubation with nuclear lysates for one hour, a STAT-3 antibody was added followed by incubation with a secondary anti-rabbit horseradish peroxidase (HRP) conjugated immunoglobulin G (IgG) antibody. Wells were washed after each incubation period. A colorimetric HRP substrate was then added. The colorimetric reaction was stopped with oxalic acid. The plate was read at 450 nm with a reference wavelength of 655nm. Each sample was assayed in duplicate, and STAT-3 nuclear activation was normalized to nuclear protein concentration.

Phosphorylated STAT-3

Phosphorylated STAT-3 was measured in cytoplasmic extracts from the ileum using a commercially available enzyme-linked immunosorbent assay (ELISA) kit following the manufacturer's suggested protocol (PathScan Phospho-STAT-3 (Tyr705) Sandwich ELISA Kit; Cell Signaling Technology, Beverly, MA). Briefly, extracts were added to individual wells of a 96- well plate coated with a STAT-3 rabbit monoclonal antibody. After overnight incubation at 4°C, the wells were washed, and a primary Phospho-STAT-3 mouse monoclonal antibody was added. After 1 hour of incubation, the wells were washed again, and a secondary anti-mouse IgG HRP conjugated antibody was added. After 30 minutes of incubation, the wells were washed, and an HRP substrate was added. After approximately 30 minutes of color development at 25°C, a stop solution was added, and the plate was read at 405 nm. Each sample was assayed in duplicated and normalized to cytoplasmic protein concentration.

NF-kappa B Nuclear Activation

Nuclear NF-kappa B activation was measured in the nuclear extracts of the ileum utilizing a commercially available transcription factor assay kit (TransAM NF-kappa B p65, Active Motif, Carlsbad, CA) following the manufacturer's suggested protocol. Briefly, nuclear extracts were added to each well of a 96 well plate in which an oligonucleotide containing the NF-kappa B consensus sequence was immobilized. After incubation with lysates, a NF-kappaB p65 antibody was added followed by incubation with a HRP conjugated secondary antibody. Wells were washed after each incubation period. A colorimetric HRP substrate was then added. The reaction was stopped with oxalic acid. The plate was read at 450 nm with a reference wavelength of 655 nm. Each sample was assayed in duplicate and normalized to total nuclear extract protein.

Myosin Light Chain Phosphorylation

Cytoplasmic extracts (50μg total protein) were separated using glycerol sodium dodecyl sulfate-polyacrylamide gel (12.5%) electrophoresis. After transfer to polyvinyldifluoride membranes, western blotting was performed by incubating the membranes with a rabbit polyclonal IgG myosin light chain antibody that recognizes the phosphorylated and unphosphorylated forms of the regulatory myosin light chain (sc-15370, 1:200 dilution, Santa Cruz Biotechnology, Santa Cruz, CA) overnight at 4°C. The membranes were subsequently incubated with a secondary anti-rabbit IgG-HRP conjugated antibody (7074, Cell Signaling Technology, Danvers, MA). Enhanced chemical luminescence was used to visualize the proteins on the membranes (ECL Plus, Amersham Biosciences, Piscataway, NJ). Quantification of bands was performed with ImageJ software (National Institutes of Health, Bethesda, MD).

Contractile Activity

Contractile activity was measured in the ileum at 6 hours in CONTROL and EDEMA groups according to methods which we have previously published. (4) Briefly, whole thickness strips were mounted in 25 mL organ baths filled with Krebs-Ringer solution (103mM NaCl, 4.7mM KCl, 2.5mM $CaCl_2$, 25mM $NaHCO_3$, 1.1mM NaH_2PO_4, and 15nM glucose). The solution was buffered with albumin to avoid edema formation during incubation in the tissue chamber and gassed with 5% CO_2-95% O_2. Isometric force was monitored by an external force displacement transducer (Quantametrics, Newtown, PA) connected to a PowerLab data acquisition system (AD Instruments, Colorado Springs, CO). Each strip was stretched to optimal length then allowed to equilibrate for at least 30 minutes prior to any measurements. After equilibration, 30 minutes of basal contractile activity data (contractile strength and frequency) was recorded. The intestinal strips were then treated with 10^{-6} M carbachol and contractile activity data recorded for 5 minutes. The dose of carbachol was based on previous dose response studies. (4)

After recording contractile activity, the strip of intestine was removed, blotted lightly, and weighed. The length of each strip was measured. The cross-sectional area of each strip was calculated from length and weight data by assuming that the density of smooth muscle was 1.05 g/cm^3. All force development was normalized to tissue cross-sectional area. Contractile activity was calculated as the area under the curve for 10 minutes. Maximally stimulated contractile activity was calculated as the area under the curve for 2 minutes immediately following carbachol treatment. Contractile frequency was measured over the same time periods

Intestinal Transit

Intestinal transit was measured according to previously published methods and determined by distribution of a nonabsorbable 70 kDa fluorescein isothiocyanate – labeled dextran (FD70). (7) Briefly, 200 μL of 2.5 mg/ml solution (dissolved in distilled water) was administered by oral gavage. After sixty minutes, the animals were sacrificed and the gastrointestinal tract was removed and divided into 11 segments (stomach and 10 equal segments of small intestine). The intraluminal contents were flushed with 2 mL of phosphate buffered saline and collected. The supernatant of the resultant samples was collected and assessed flourometrically for concentration of FD70. Transit was evaluated by calculating the geometric center of distribution of FD60 (Σ ((fluorescent signal per segment (percent) x segment number)/100).

Statistics

Unless otherwise stated, all values are presented as mean ± standard error of the mean (SEM). For data that was compared over multiple timepoints, a 2-way analysis of variance (ANOVA) was utilized to determine statistically significant differences. If differences were noted, a 2 tailed unpaired t-test was used for comparisons between groups. For all other data, a 2 tailed unpaired t-test was utilized. A p value of < 0.05 was utilized to denote statistical significance.

Results

Acute Mesenteric Venous Hypertension

Superior mesenteric vein constriction led to a significant increase in baseline mesenteric pressures. The pressure post-constriction was 10 ± 1 mmHg as compared to 2 ± 1 mmHg when measured at baseline (n=3).

Wet to Dry Ratio

The combination of mesenteric venous hypertension and high volume crystalloid administration resulted in significant development of edema at 30 minutes (3.16 ± 0.06 versus 4.18 ± 0.15, CONTROL (n=7) versus EDEMA (n=8)), 2 hours (3.49 ± 0.05 versus 4.42 ± 0.10, CONTROL (n=7) versus EDEMA (n=7)), and 6 hours (3.42 ± 0.05 versus 3.94 ± 0.04, CONTROL (n=7) versus EDEMA (n=8)) (Figure 1a). Values are expressed as a unitless ratio.

Myeloperoxidase Activity

Myeloperoxidase activity was measured at 30 minutes, 2 hours, and 6 hours. There was no difference in activity at 30 minutes (0.044 ± 0.009 versus 0.056 ± 0.012, CONTROL (n=6) versus EDEMA (n=7)), 2 hours (0.018 ± 0.002 versus 0.019 ± 0.002, CONTROL (n=7) versus EDEMA (n=7)), or 6 hours (0.019 ± 0.004 versus 0.026 ± 0.004, CONTROL (n=6) versus EDEMA (n=8)) (Figure 1b). Values are expressed as absorbance per microgram protein.

Chiu Scoring

Chiu scoring (to quantitate mucosal damage) was measured in the ileum at 6 hours. As determined by a blinded observer, the Chiu score was 1 ± 0 for CONTROL animals (n=5) and 1 ± 0 for EDEMA groups (n=4). Values are expressed as a unitless number. Representative images are demonstrated in Figure 2.

STAT-3 Nuclear Activation

STAT-3 nuclear activation was measured in the ileum at 30 minutes, 2 hours and 6 hours. There was no difference between CONTROL (0.13 ± 0.01, n=6) and EDEMA (0.13 ± 0.02, n=7) groups at 30 minutes. However, at 2 hours (0.10 ± 0.01 versus 0.18 ± 0.02, CONTROL (n=6) versus EDEMA (n=7)) and 6 hours (0.13 ± 0.01 versus 0.19 ± 0.01, CONTROL (n=5) versus EDEMA (n=7)), a significant increase in STAT-3 nuclear activation was noted in the EDEMA groups (Figure 3a). Values are expressed as absorbance per microgram protein.

Phosphorylated STAT-3

Levels of phosphorylated STAT-3 were measured in the ileum at 30 minutes, 2 hours and 6 hours. There was no significant difference in levels of phosphorylated STAT-3 at 30 minutes (0.10 ± 0.01 versus 0.10 ± 0.01, CONTROL (n=6) versus EDEMA (n=7)) or 2 hours (0.13 ± 0.01 versus 0.17 ± 0.03, CONTROL (n=6) versus EDEMA (n=7)). However, at 6 hours, levels of phosphorylated STAT-3 was significantly increased in the EDEMA group (0.20 ± 0.01, n=5) as compared to CONTROL (0.14 ± 0.02, n=8) (Figure 3b). Values are expressed as absorbance per microgram protein.

NF-kappa B Nuclear Activation

Similar to STAT-3 nuclear activation, levels of NF-kappa B nuclear activation were determined in the ileum at 30 minutes, 2 hours, and 6 hours. At 30 minutes, there was no difference in NF-kappa B nuclear activation (0.24 ± 0.3 versus 0.22 ± 0.03, CONTROL (n=6) versus EDEMA (n=7)). There was significantly higher NF-kappa B nuclear activation at 2 hours (0.09 ± 0.01 versus 0.13 ± 0.01, CONTROL (n=6) versus EDEMA (n=7)). At 6 hours, NF-kappa B nuclear binding continues to be significantly elevated in the EDEMA group (0.03 ± 0.00, n=5) versus CONTROL (0.02 ± 0.00, n=8) (Figure 3c). Values are expressed as absorbance per microgram protein.

Myosin Light Chain Phosphorylation

Hydrostatic edema resulted in a significant decrease in the phosphorylated fraction of myosin light chain (0.86 ± 0.02 versus 0.76 ± 0.03, CONTROL (n=4) versus EDEMA (n=4)). Values are expressed as the unitless ratio of phosphorylated myosin light chain to total myosin light chain. A representative western blot is demonstrated in Figure 4.

Contractile Function

The induction of hydrostatic edema significantly decreased both basal (14.4 ± 1.8 versus 4.9 ± 1.2, CONTROL versus EDEMA) and maximally stimulated (carbachol) (28.5 ± 3.2 versus 9.5 ± 2.4, CONTROL versus EDEMA) contractile activity (n=8 (CONTROL) and n=6 (EDEMA)). There was no significant difference in either baseline or maximally stimulated contractile frequency between CONTROL and EDEMA groups (DATA NOT SHOWN). All contractile function testing was performed at the 6 hour time point. Contractile strength is expressed as stress ($g/cm^2/s$). Representative contractile tracings are demonstrated in Figure 5.

Intestinal Transit

Edema significantly decreased small intestinal transit. The calculated geometric center of CONTROL animals (5.10 ± 0.33, n=6) was significant higher than that of EDEMA animals (3.24 ± 0.63, n=6). There was no significant difference in gastric emptying rate noted between animals (63 ± 3% versus 49 ± 8%, CONTROL versus EDEMA, p=0.2).

Discussion

The combination of high volume resuscitation and mesenteric venous hypertension (as a surrogate to abdominal packing) in mice leads to development of significant intestinal edema and resultant intestinal contractile dysfunction. This occurs in the absence of factors generally associated with neutrophil mediated inflammation and ischemia/reperfusion mediated mucosal injury and is associated with a signal transduction profile often attributed to models of inflammation and systemic (i.e., hemorrhagic shock/resuscitation) and/or regional (i.e., superior mesenteric artery occlusion) ischemia/reperfusion mediated injury.

Superior mesenteric vein constriction led to acute induction of mesenteric venous hypertension. Venous hypertension has been noted in models of intra-abdominal hypertension and abdominal compartment syndrome and is believed to contribute to intestinal edema by increasing tissue hydrostatic forces. The increase in magnitude in this model appears to correlate with previously published data.(8–10)

Most models used to study intestinal contractile dysfunction in the setting of trauma rely on some type of ischemia/reperfusion injury or bowel manipulation with resultant mucosal injury. (5, 11–13) In this model, we demonstrate that edema in a setting of little to no mucosal injury leads to contractile dysfunction. The contractile dysfunction is associated with increases in STAT-3 and NF-kappa B activity, similar to what is seen in ischemia/reperfusion and bowel manipulation models. (14, 15) Intestinal edema is often viewed as an inevitable consequence of both pathology and treatment. The data presented support the notion that edema may function as an amplifier and/or initiator of dysfunctional signaling cascades, culminating in intestinal contractile dysfunction.

Development of a mouse model is a natural extension of our previously published work in resuscitation-induced intestinal edema and resultant contractile dysfunction. Most importantly, it allows for the use of constitutional and conditional knock-out models to further our understanding of the importance of various elements in the regulation of intestinal contractile function, confirm the effect (or lack of effect) of hydrostatic edema, and further the identification of potential targets of novel therapies.

In this model, we used a combination of mesenteric venous hypertension with high volume crystalloid resuscitation. Perturbed microvascular fluid exchange as determined by hydrostatic and colloid oncotic pressures is of paramount importance in the development of intestinal edema formation and is described by the Starling equation. (16) High volume crystalloid resuscitation and abdominal packing serves to alter hydrostatic and oncotic pressures, leading to net accumulation of tissue water in multiple organ systems. High volume crystalloid resuscitation decreases plasma oncotic pressures and abdominal (specifically peri-hepatic) packing, as a component of damage control resuscitation, increases mesenteric venous pressures, leading to increased capillary hydrostatic pressures. Decreased plasma oncotic pressure and increased capillary pressure both favor movement of fluid from the vasculature into the interstitium.

We did not examine the effects of fluid resuscitation and venous hypertension alone in this model for several reasons. We have previously shown in rats that high volume crystalloid resuscitation alone or venous hypertension alone does not lead to development of significant intestinal edema with resultant contractile dysfunction. (2, 4) This is true for measurements of intestinal contractility and transit as well as published mediators of the intestinal contractile complex, such as STAT-3 and NF-kappa B. (17, 18)

In this manuscript, we evaluated intestinal contractility as an ex-vivo marker for intestinal transit. We have shown previously that intestinal contractility is the functional correlate for

intestinal transit measurements. (4) Measuring intestinal contractility as a marker for transit in mice offers the opportunity to evaluate the effect of pharmacological manipulation on various factors affecting contractile function. We additionally demonstrate that the decrease in intestinal contractility leads to the functional result of decreased intestinal transit. Although a valid criticism of the method used to measure intestinal transit in this manuscript is the dependence on gastric emptying, we demonstrate no significant difference in gastric emptying rate between the two experimental groups.

In previous work, contractility and transit studies have been measured from 6 to 24 hours following induction of intestinal edema. (2) The maximum effect on transit appears to be between 6 and 12 hours. We have increasingly noted the potential role of early mechanical changes to the pathogenesis of intestinal edema. (3, 4, 19–23) The 6-hour timepoint allows us the ability to examine potential contributions of mechanical changes on intestinal contractility and transit which may be initiators for signal transduction cascades culminating in intestinal contractile dysfunction. (23)

In summary, we have developed a novel murine model for the study of intestinal edema and subsequent contractile dysfunction. The elimination of factors classically associated with inflammation and ischemia/reperfusion injury, such as neutrophil infiltration and mucosal injury allows us to target the signal transduction cascades affected by edema alone and further clarifies the importance of intestinal edema as a potential initiation and/or propagator of dysfunctional signaling pathways leading to the functional endpoint of ileus.

Acknowledgments

SOURCES OF SUPPORT: NIH Grants RO1 HL 092916, P50 GM 38529, T32 GM 0879201, and KO1 DK 070758

References

1. Moore-Olufemi SD, Xue H, Allen SJ, et al. Inhibition of intestinal transit by resuscitation-induced gut edema is reversed by L-NIL. J Surg Res. 2005; 129:1–5. [PubMed: 15978623]
2. Moore-Olufemi SD, Xue H, Attuwaybi BO, et al. Resuscitation-induced gut edema and intestinal dysfunction. J Trauma. 2005; 58:264–270. [PubMed: 15706186]
3. Radhakrishnan RS, Xue H, Weisbrodt N, et al. Resuscitation-induced intestinal edema decreases the stiffness and residual stress of the intestine. Shock. 2005; 24:165–170. [PubMed: 16044088]
4. Uray KS, Laine GA, Xue H, Allen SJ, Cox CS Jr. Intestinal edema decreases intestinal contractile activity via decreased myosin light chain phosphorylation. Crit Care Med. 2006; 34:2630–2637. [PubMed: 16915113]
5. Attuwaybi B, Kozar RA, Gates KS, et al. Hypertonic saline prevents inflammation, injury, and impaired intestinal transit after gut ischemia/reperfusion by inducing heme oxygenase 1 enzyme. J Trauma. 2004; 56:749–758. discussion 758–749. [PubMed: 15187737]
6. Chiu CJ, McArdle AH, Brown R, Scott HJ, Gurd FN. Intestinal mucosal lesion in low-flow states. I. A morphological, hemodynamic, and metabolic reappraisal. Arch Surg. 1970; 101:478–483. [PubMed: 5457245]
7. Nakao A, Schmidt J, Harada T, et al. A single intraperitoneal dose of carbon monoxide-saturated ringer's lactate solution ameliorates postoperative ileus in mice. J Pharmacol Exp Ther. 2006; 319:1265–1275. [PubMed: 16943253]
8. Rasmussen IB, Berggren U, Arvidsson D, Ljungdahl M, Haglund U. Effects of pneumoperitoneum on splanchnic hemodynamics: an experimental study in pigs. Eur J Surg. 1995; 161:819–826. [PubMed: 8749214]
9. Balogh Z, McKinley BA, Cox CS Jr, et al. Abdominal compartment syndrome: the cause or effect of postinjury multiple organ failure. Shock. 2003; 20:483–492. [PubMed: 14625470]

10. Shah SK, Jimenez F, Walker PA, et al. A novel physiologic model for the study of abdominal compartment syndrome (ACS). J Trauma. 68:682–689. [PubMed: 20220423]
11. Kalff JC, Schraut WH, Simmons RL, Bauer AJ. Surgical manipulation of the gut elicits an intestinal muscularis inflammatory response resulting in postsurgical ileus. Ann Surg. 1998; 228:652–663. [PubMed: 9833803]
12. Hassoun HT, Weisbrodt NW, Mercer DW, Kozar RA, Moody FG, Moore FA. Inducible nitric oxide synthase mediates gut ischemia/reperfusion-induced ileus only after severe insults. J Surg Res. 2001; 97:150–154. [PubMed: 11341791]
13. Hierholzer C, Kalff JC, Chakraborty A, et al. Impaired gut contractility following hemorrhagic shock is accompaied by IL-6 and G-CSF production and neutrophil infiltration. Dig Dis Sci. 2001; 46:230–241. [PubMed: 11281168]
14. Hierholzer C, Kalff JC, Audolfsson G, Billiar TR, Tweardy DJ, Bauer AJ. Molecular and functional contractile sequelae of rat intestinal ischemia/reperfusion injury. Transplantation. 1999; 68:1244–1254. [PubMed: 10573059]
15. Wehner S, Schwarz NT, Hundsdoerfer R, et al. Induction of IL-6 within the rodent intestinal muscularis after intestinal surgical stress. Surgery. 2005; 137:436–446. [PubMed: 15800492]
16. Staub, NC.; Taylor, AE. Edema. New York: Raven Press; 1984.
17. Uray KS, Laine GA, Xue H, Allen SJ, Cox CS Jr. Edema-induced intestinal dysfunction is mediated by STAT3 activation. Shock. 2007; 28:239–244. [PubMed: 17515852]
18. Uray K, Cox C, Laine G. Analysis of intestinal smooth muscle genes induced by intestinal edema for common regulatory elements. Shock. 2009; 31:87. [PubMed: 18497710]
19. Cox CS Jr, Radhakrishnan R, Villarrubia L, et al. Hypertonic saline modulation of intestinal tissue stress and fluid balance. Shock. 2008; 29:598–602. [PubMed: 18414233]
20. Radhakrishnan RS, Shah SK, Lance SH, Radhakrishnan HR, Xue H, Radhakrishnan GL, Ramaswamy U, Walker PA, Laine GA, Stewart RH, Cox CS. Hypertonic saline alters hydraulic conductivity and up-regulates mucosal/submucosal aquaporin 4 in resuscitation-induced intestinal edema. Crit Care Med. 2009 In press.
21. Radhakrishnan RS, Radhakrishnan HR, Xue H, et al. Hypertonic saline reverses stiffness in a Sprague-Dawley rat model of acute intestinal edema, leading to improved intestinal function. Crit Care Med. 2007; 35:538–543. [PubMed: 17205008]
22. Radhakrishnan RS, Xue H, Moore-Olufemi SD, et al. Hypertonic saline resuscitation prevents hydrostatically induced intestinal edema and ileus. Crit Care Med. 2006; 34:1713–1718. [PubMed: 16625118]
23. Shah SK, Fogle LN, Aroom KR, Gill BS, Moore-Olufemi SD, Jimenez F, Uray KS, Walker PA, Stewart RH, Laine GA, Cox CS. Hydrostatic edema induced signaling pathways: potential role of mechanical forces. Surgery. 2010 In press.

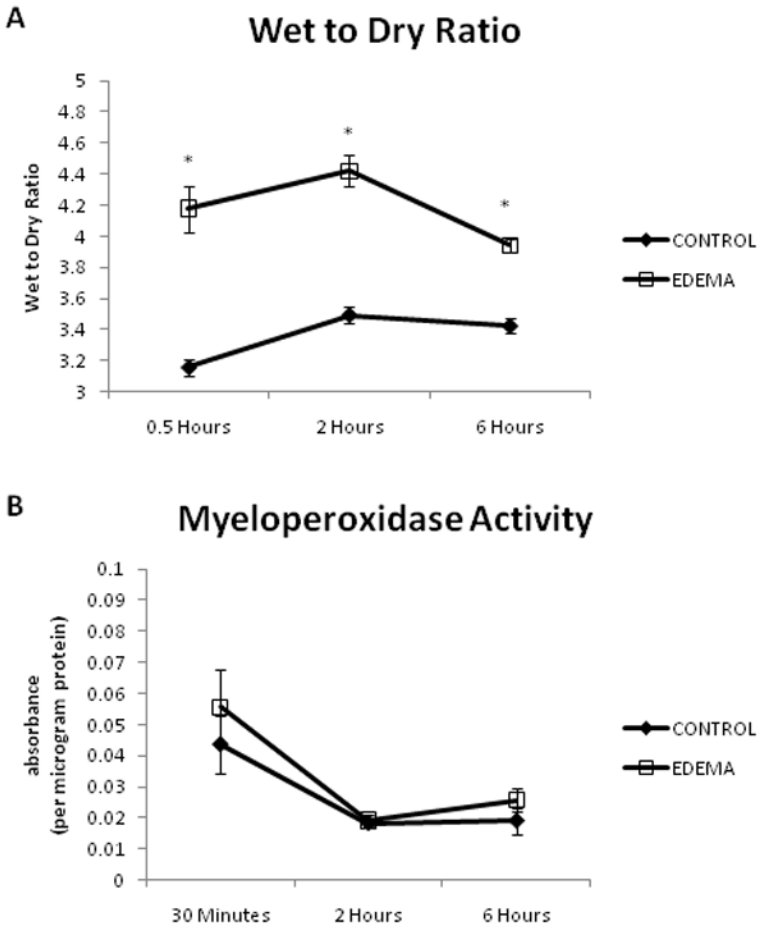

Figure 1.

There is a significantly higher wet to dry ratio at 30 minutes to 6 hours in the EDEMA groups as compared to CONTROL groups without a change in myeloperoxidase level. An n of 6–7 was used for all CONTROL animals and an n of 7–8 was used for all EDEMA animals. (* represents statistical difference ($p<0.05$) between CONTROL and EDEMA groups; (a) wet to dry ratios, (b) myeloperoxidase activity)

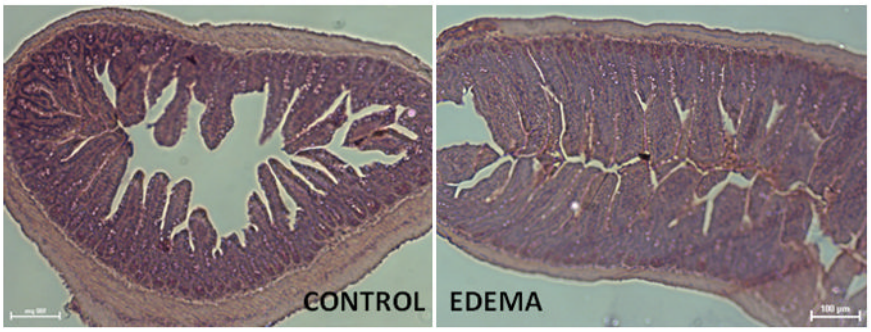

Figure 2.
Representative H&E stained images from CONTROL and EDEMA groups are demonstrated. There is no significant mucosal damage to indicate ischemia/reperfusion injury. All images are at 10x magnification and the scale bar represents 100μm.

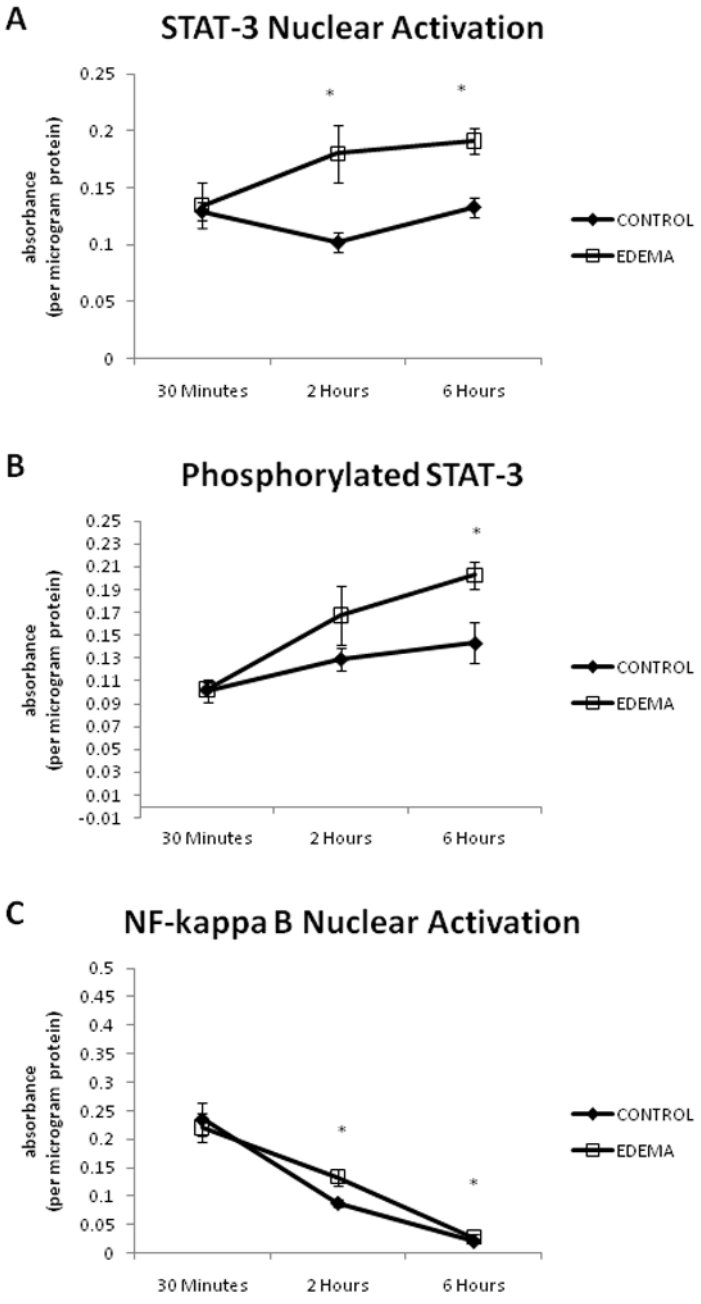

Figure 3.

EDEMA causes significant increases in STAT-3 and NF-kappa B nuclear activation as well as in the levels of phosphorylated STAT-3. An n of 5–7 was used for all CONTROL groups and an n of 7–8 was used for all EDEMA groups. (* represents statistical difference ($p<0.05$) between CONTROL and EDEMA groups; (a) STAT-3 nuclear activation, (b) phosphorylated STAT-3, (c) NF-kappa B nuclear activation)

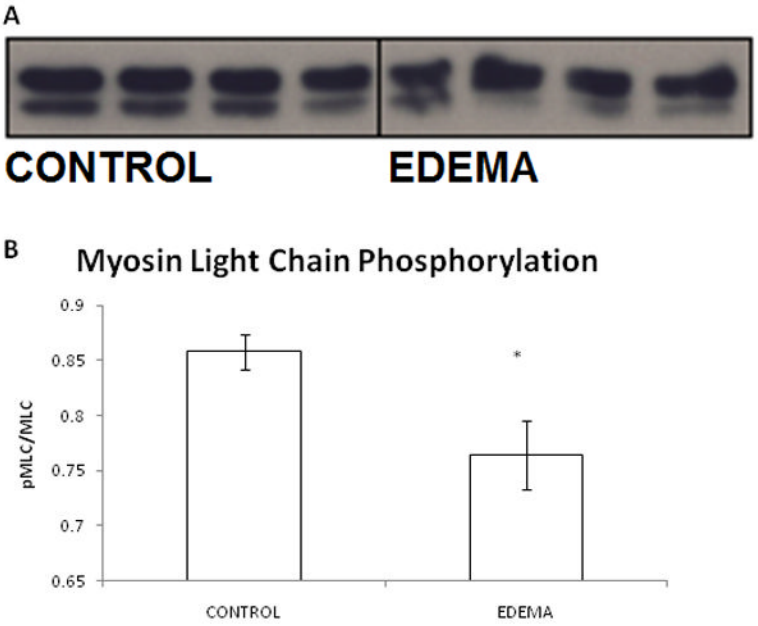

Figure 4.

Representative western blot with image quantification analysis from CONTROL and EDEMA mice. Hydrostatic edema causes a significant decrease in phosphorylated myosin light chain, the obligatory step in the smooth muscle contractile pathway. An n of 4 was used for CONTROL and EDEMA groups. (* represents statistical difference ($p<0.05$) between CONTROL and EDEMA groups; (a) representative western blot, (b) image quantification analysis

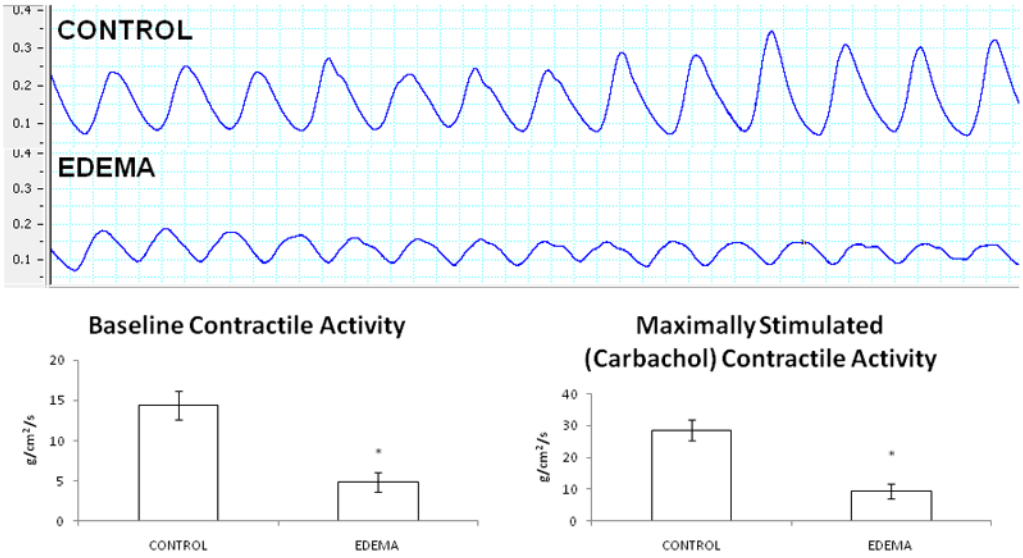

Figure 5.

Representative basal contractile activity tracing from CONTROL and EDEMA mice. Each box represents 2 seconds. Note the significantly decreased contractile strength in the EDEMA animals. An n of 8 was used for the CONTROL group and an n of 6 was used for the EDEMA group. (* represents statistical difference ($p<0.05$) between CONTROL and EDEMA groups)